Journal of Marine Science and Technology
https://doi.org/10.1007/s00773-024-01020-4

ORIGINAL ARTICLE

Nonlinear steering control law under input magnitude and rate constraints with exponential convergence

Rin Suyama[1] · **Satoshi Satoh**[1] · **Atsuo Maki**[1]

Received: 24 October 2023 / Accepted: 25 July 2024

Abstract
A ship steering control law is designed for a nonlinear maneuvering model whose rudder manipulation is constrained in both magnitude and rate. In our method, the tracking problem of the target heading angle with input constraints is converted into the tracking problem for a strict-feedback system without any input constraints. To derive this system, hyperbolic tangent (tanh) function and auxiliary variables are introduced to deal with the input constraints. Furthermore, using the feature of the derivative of tanh function, auxiliary systems are successfully derived in the strict-feedback form. The backstepping method is utilized to construct the control input for the resulting cascade system. The proposed steering control law is verified in numerical experiments, and the result shows that the tracking of the target heading angle is successful using the proposed control law.

Keywords Ship steering control · Exponential stability · Input magnitude constraint · Input rate constraint · Backstepping

1 Introduction

Ship is one of the transportations that handles the mass transportation of cargo and passengers, and technology for the safe navigation of ships is an important research issue. In many cases, ships navigating the oceans utilize steering control laws. In the case the target heading angle is a time-invariant constant, the control laws are often referred to as course keeping control [1, 2].

Response models of ship maneuvering motion and steering control laws based on them have long been studied. The research on steering control started with the study using Proportional-Integral control in [3]. Proportional-Derivative control in [4] is also well known. Nomoto's study [5] was the first to consider such a ship course control from the system control point of view. In this study, the maneuvering model of a ship was represented as a first-order or second-order system. In particular, the first-order model is widely used as the *Nomoto's KT model*, for instance, to evaluate the maneuverability of new ships in ship building companies. In the literature [2], the steering control was designed using the model reference adaptive control technique. In the literature [6], sliding mode control (SMC) was adopted in the design of the steering control, and the design parameters included in the designed control law were optimized based on the genetic algorithm. In the literature [7], the steering control for a maneuvering model with time-varying uncertain parameters, including control coefficient, was designed using the adaptive backstepping method.

In a ship maneuvering mechanism, there are constraints on the manipulation of the actuators such as rudders and propellers. These input constraints are due to the mechanics of the actuators. Therefore, all ships are subject to the actuator constraints. These input constraints can be divided into magnitude constraint and rate constraint [8, 9]. Closed loop systems may become unstable in the case the constraints on the input magnitude are not properly treated [8]. In the case rate constraint exists, it has been observed that the controlled system may continue to oscillate, which can be understood as a kind of self-excited oscillation, and in the worst case, the system becomes uncontrollable. The degradation of control laws due to input constraints is exemplified in Fig. 2. In the controlled system shown in Fig. 2, the same control law

✉ Rin Suyama
suyama_rin@naoe.eng.osaka-u.ac.jp

Satoshi Satoh
satoh@mech.eng.osaka-u.ac.jp

Atsuo Maki
maki@naoe.eng.osaka-u.ac.jp

[1] Osaka University, 2-1 Yamadaoka, Suita, Osaka, Japan

Published online: 28 August 2024

was implemented to track the target signal. From Fig. 2, it can be observed that even if a control law can achieve the tracking of a target signal without input constraints, it may fail in the tracking control in the case it is implemented in a system subject to input constraints. This will lead to serious accidents, such as the one illustrated in Fig. 1. Also in the field of aircraft control, oscillation phenomena caused by input rate saturation are known as Pilot-Induced Oscillation (PIO) in Category II [10] and have been analyzed [9].

Various methods have been studied to control systems with input constraints. In the control of a system with input magnitude constraint, the anti-windup technique is well known [11, 12]. In the literature [13], a tracking control law was designed for a nonlinear system with an input magnitude constraint and unknown system parameters. This study was extended to the system with external disturbance by introducing hyperbolic tangent (tanh) function as a smooth approximation for saturation nonlinearity and using the backstepping method in the literature [14]. In the literature [15], stabilizing control laws were designed using SMC for a linear system with constraints on input magnitude and rate. In the literature [16], the constant bearing (CB) guidance [17] was applied to bound signals in the controlled system, and it was shown that Multi-Input Multi-Output (MIMO) ship dynamic positioning is possible with smaller input by including CB guidance into the backstepping procedure. In the literature [18], a control law was designed for aircraft maneuvering motion represented by a linear system with

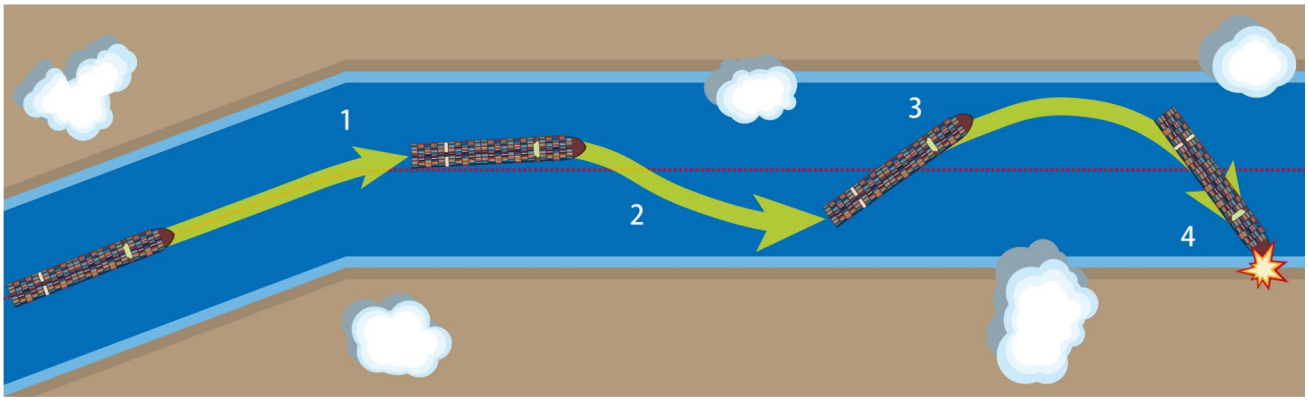

Fig. 1 An example of the mechanism of allision/collision accidents due to the constraints on rudder manipulation; 1. The control law sends the rudder command to follow the target path. However, the response of maneuvering motion delays due to the constrained manipulation of the steering system. 2. Tracking error remains, so the control law continues to command the steering system to turn right. As a result, overshoot occurs. 3. The control law attempts to recover from the overshoot and commands a left turn, but again the constraints on the rudder angle and the steering speed cause a delay in the response of the maneuvering motion. 4. Overshooting occurs continuously and, in the worst case, is amplified, leading to an allision/collision

Fig. 2 An example of the degradation of a control law due to input magnitude and rate constraints

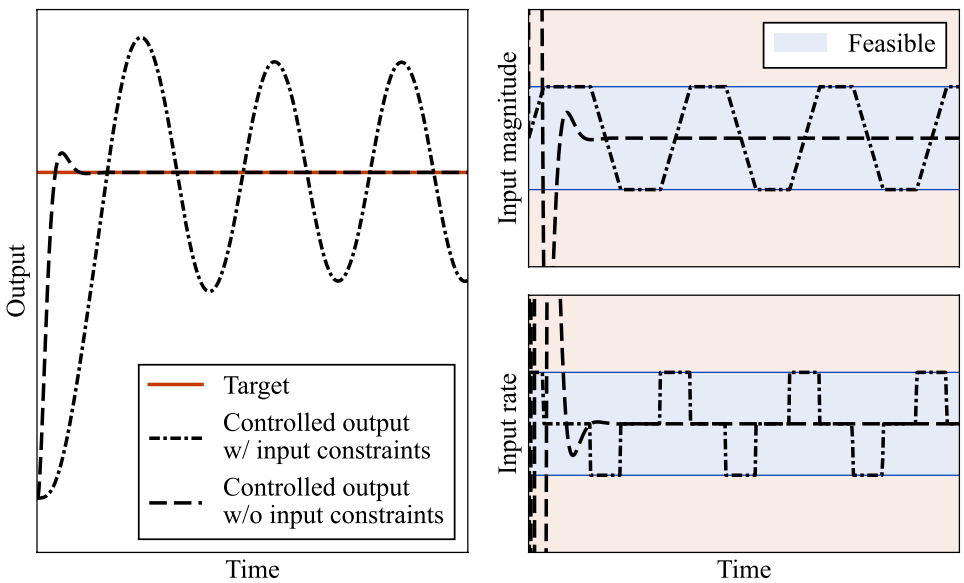

elliptical constraints on input magnitude and rate, and it achieved bounded tracking error. In the framework of optimal control, constraints on input magnitude and rate can be formulated easily. In the literature [19], in the framework of the dynamic window approach, the constraints of both input magnitude and rate were considered in the computation of feasible velocity states. In the literature [20], reinforcement learning was utilized to train the path tracking controller for airships. In the framework of the reinforcement learning of this work, to treat input constraints, actuator states and their rate were handled as a part of the state variable and the action, respectively. Although a variety of efforts can be found as listed here, the authors have not found studies that have designed tracking control laws for nonlinear systems with constrained input magnitude and rate and discussed the convergence of the tracking error.

In the field of ship steering control, some methods to deal with the constraints on rudder manipulation have also been studied. In the literature [21], in addition to the nonlinear maneuvering model, the system of the rudder manipulation was taken into account as a first-order system in the design of the steering control. In the literature [22], adaptive steering control was designed with a linear quadratic controller and Riccati based anti-windup compensator. In the literature [23], SMC was applied to design a steering control for the system with input magnitude constraint, and the asymptotical stability was established. Furthermore, in this study, design parameters were adjusted based on fuzzy theory to avoid the chattering of the control signal. The work [7] was extended in [24] to the case with the external disturbance and the rudder magnitude constraint. In the literature [25], a finite-time adaptive output feedback steering control was designed based on a fuzzy logic system for a nonlinear maneuvering system with input magnitude constraint. However, these steering control laws did not explicitly address the rate constraint of the rudder manipulation.

Some reference shaping methods were proposed for the avoidance of input magnitude and rate saturation. Reference filter [26] makes the reference signal smooth, and, by incorporating saturation elements, explicitly limits the velocity/acceleration of the reference signal. In ship course control, for instance, the reference filter makes it possible to avoid actuator magnitude and rate saturation by shaping the reference signal that changes smoothly from the current heading angle to the target heading angle. If the reference can be smoothed sufficiently, the performance of the applied control law, e.g., exponential stability, will not be degraded. However, the reference signal smoothed by the reference filter does not guarantee that the output of the control law will satisfy the constraints at any state. In addition, since the velocity and acceleration are clipped to fixed values, it is not always possible to control the actuator to its limits, in terms of magnitude and rate, considering the current state. Therefore, the control method using the reference filter does not allow the actuators to be manipulated to their full extent. Reference governor [27] was designed for the controlled system with state and input constraints, and can shape the reference signal for the avoidance of violence of these constraints. In this method, nonlinear optimization problems must be solved online, taking into account state constraints in addition to input constraints, and, generally, implementation can be burdensome. In summary, at this stage, for the nonlinear system with constraints of input magnitude and rate, the development of tracking control laws that make the closed loop system exponentially stable has not been achieved. In addition, the reference filter and the reference governor for the treatment of input constraints are incomplete or expensive to implement.

Motivated by the above problems, this study focuses on a tracking control law that does not require shaping of the reference signal and guarantees satisfaction of the input magnitude and rate constraints. The contribution of this study is the design of a steering control law which has the following features:

- a nonlinear response model of maneuvering motion is targeted,
- both constraints of rudder angle and steering speed are guaranteed to be satisfied,
- the tracking error is made to exponentially converge to the origin.

In our method, the tracking problem of the target heading angle with input constraints is transformed into the regulation problem for an error system which is described in a strict-feedback form without any input constraints. To derive such a system, the authors introduce hyperbolic tangent (tanh) function and auxiliary variables to deal with the constraints on input as some existing method [14, 25, 28, 29]. Furthermore, by a time derivative of the formulated variable, due to the feature of the derivative of tanh function, an auxiliary system for rudder manipulation is constructed in the strict-feedback form. Using this technique two times, for the constraints of magnitude and rate, respectively, both actuator constraints are successfully incorporated into the cascade system which does not have any input constraints. The control input is designed using the backstepping technique [30, 31] for the resulting strict-feedback system. Although the proposed steering control law has a limitation in terms of numerical implementation, it is the first attempt at the tracking control for nonlinear systems under input magnitude and rate saturations with exponential convergence. To verify the proposed control law, numerical experiments are conducted.

The rest of the paper is organized as follows: Sect. 2 describes the notation used in this manuscript; Sect. 3 describes the tracking problem of the target heading angle

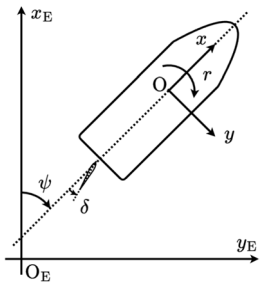

Fig. 3 Coordinate systems

considered in this study; Sect. 4 describes the conventional method and the design procedure of the proposed control law; Sect. 5 describes the numerical experiments implemented to verify the proposed steering control law and compare the performance with the conventional method; Sect. 6 discusses the property of the proposed method in terms of the unboundedness of control signal point of view; finally, Sect. 7 concludes the study.

Initial results from the investigation presented in this study were initially described in [32]. In this paper, the results are presented more extensively, with more details, and with some revisions.

2 Notation

$\mathbb{R}$ represents the set of all real numbers. $\mathbb{R}^n$ represents the n-dimensional Euclidean space. $\mathbb{R}_+$ represents the set of all positive real numbers. $|x|$ represents the absolute value of $x \in \mathbb{R}$. The overdot " $\dot{}$ " represents the derivative with respect to time t. The saturation function $\mathrm{sat}(s, \bar{s})\colon \mathbb{R} \times \mathbb{R}_+ \to [-\bar{s}, \bar{s}]$ is defined as:

$$\mathrm{sat}(s, \bar{s}) := \begin{cases} s & \text{for} \quad |s| \le \bar{s}, \\ \mathrm{sgn}(s)\bar{s} & \text{for} \quad |s| > \bar{s}. \end{cases} \tag{1}$$

$\mathrm{diag}(a_1, \ldots, a_n)$ represents a diagonal matrix $A \in \mathbb{R}^{n\times n}$ such that:

$$A_{ij} := \begin{cases} a_i & \text{for } i = j, \\ 0 & \text{for } i \ne j. \end{cases} \tag{2}$$

3 Problem formulation

3.1 Maneuvering model

The ship is assumed to move on an Earth-fixed coordinate $\mathrm{O_E} - x_\mathrm{E} y_\mathrm{E}$ as Fig. 3 shows. $\psi(t)$, $r(t)$, and $\delta(t)$ represent the heading angle, yawing angular velocity, and rudder angle, respectively. $\mathrm{O} - xy$ in Fig. 3 represents a body-fixed coordinate system with the origin on the center of the ship.

The heading angle $\psi(t)$ and the yawing angular velocity $r(t)$ follow Eq. 3.

$$\dot{\psi}(t) = r(t) \ . \tag{3}$$

In this study, it is assumed that the change in ship speed due to turning motion is insignificant. Thus, the ship speed is assumed to be constant. In this situation, it is known that the maneuvering motion of a ship can be modeled by the following single-input single-output (SISO) state equation:

$$\dot{r}(t) = f(r(t)) + b\delta(t), \tag{4}$$

where $f\colon \mathbb{R} \to \mathbb{R}$ is a two times differentiable function, $b \ne 0$. Well-known examples of this formulation are the linear system (Nomoto's KT model) [5]:

$$\begin{aligned} &T\dot{r}(t) + r(t) = K\delta(t) \\ &\Leftrightarrow \dot{r}(t) = -\frac{1}{T}r(t) + \frac{K}{T}\delta(t), \end{aligned} \tag{5}$$

and the system expressed by three-dimensional polynomial of $r(t)$ [33]:

$$\begin{aligned} &T\dot{r}(t) + H(r) = K\delta(t) \\ &\Leftrightarrow \dot{r}(t) = -\frac{1}{T}H(r(t)) + \frac{K}{T}\delta(t), \end{aligned} \tag{6}$$

where $K \ne 0$, $T \ne 0$, $H\colon \mathbb{R} \to \mathbb{R}$ is a function of r which is defined as:

$$H(r) = n_3 r^3 + n_2 r^2 + n_1 r + n_0 \tag{7}$$

with constants $n_i \in \mathbb{R}$ $(i = 0, 1, 2, 3)$.

3.2 Constraints on rudder manipulation

It is customary for actual control systems, including ships, to have constraints on their input. In this study, as constraints on rudder angle $\delta(t)$ and rudder manipulation speed $\dot{\delta}(t)$, the following inequalities are considered:

$$|\delta(t)| \le M \quad \forall t, \tag{8}$$

$$|\dot{\delta}(t)| \le R \quad \forall t, \tag{9}$$

where $M > 0$ and $R > 0$ are constants.

The formulations Eqs. 8 and 9 are reasonable as constraints imposed on the rudder manipulation system of ships. In a typical rudder manipulation system, the rudder angle is restricted to an interval symmetrical from the origin, for instance to $[-35, 35]$ degree, which can be expressed by Eq. 8. The constraint on the rudder manipulation speed must be expressed in the formulation that it always does not exceed a certain

threshold value. In the design procedure of ship controllers, the constraint on rudder manipulation speed is often treated by introducing a first-order system [21, 34] of rudder angle $\delta(t)$ with the commanded rudder angle $\delta_c(t)$ as the input:

$$\dot{\delta}(t) = \frac{1}{T_R}(K_R\delta_c(t) - \delta(t)), \tag{10}$$

where $T_R > 0$ and $K_R > 0$ are constants. Under this formulation, $\dot{\delta}(t)$ depends on the deviation between the rudder angle $\delta(t)$ and the commanded rudder angle $\delta_c(t)$. Therefore, the values of T_R and K_R must be adjusted to moderate the rudder manipulation speed to guarantee the satisfaction of constraint Eq. 9. However, if the rudder manipulation is slowed to the extent that the satisfaction of constraint Eq. 9 is guaranteed for any $|\delta(t)| \leq M$ and $|\delta_c(t)| \leq M$, the response of $\delta(t)$ will be too slow that the model is inappropriate. In the proposed method, the constraint Eq. 9 is directly addressed instead of assuming the first-order system of rudder manipulation Eq. 10.

3.3 Desired heading angle

The target heading angle $\psi^d(t)$ is assumed to be given as the function of time t. Here, it is assumed that $\psi^d(t)$ is four times differentiable.

It is assumed that the time series $\psi^d(t)$ is feasible under constraints Eqs. 3, 4, 8 and 9. For instance, if $\psi^d(t)$ includes an oscillation with high frequency, the exponential stabilization of the tracking error for this $\psi^d(t)$ is unachievable. Thus, such a $\psi^d(t)$ is out of the scope of this study. The condition for $\psi^d(t)$ to be feasible is derived as follows. Equation 4 gives:

$$\delta(t) = \frac{\dot{r}(t) - f(r(t))}{b}, \tag{11}$$

$$\dot{\delta}(t) = \frac{1}{b}\left(\ddot{r}(t) - \frac{\mathrm{d}f}{\mathrm{d}r}(r(t))\dot{r}(t)\right). \tag{12}$$

With these, canceling $\delta(t)$ and $\dot{\delta}(t)$ in Eqs. 8 and 9, the followings are obtained:

$$\left|\frac{\dot{r}(t) - f(r(t))}{b}\right| \leq M \quad \forall t, \tag{13}$$

$$\left|\frac{1}{b}\left(\ddot{r}(t) - \frac{\mathrm{d}f}{\mathrm{d}r}(r(t))\dot{r}(t)\right)\right| \leq R \quad \forall t, \tag{14}$$

Now, $r^d(t) := \dot{\psi}^d(t)$ is defined. In Eqs. 13 and 14, letting $r(t) \leftarrow r^d(t), \dot{r}(t) \leftarrow \dot{r}^d(t), \ddot{r}(t) \leftarrow \ddot{r}^d(t)$, the conditions on $r^d(t)$ are obtained as:

$$\left|\frac{\dot{r}^d(t) - f(r^d(t))}{b}\right| \leq M \quad \forall t, \tag{15}$$

$$\left|\frac{1}{b}\left(\ddot{r}^d(t) - \frac{\mathrm{d}f}{\mathrm{d}r}(r^d(t))\dot{r}^d(t)\right)\right| \leq R \quad \forall t. \tag{16}$$

Eqs. 15 and 16 are the necessary conditions for the exact tracking of $\psi^d(t)$. Thus, $\psi^d(t)$ that does not satisfy Eqs. 15 and 16 is out of the scope of this study.

3.4 Control objective

The tracking error:

$$e_\psi(t) := \psi(t) - \psi^d(t) \tag{17}$$

is defined. The goal of the control law designed in this study is to achieve the exponential convergence of the tracking error $e_\psi(t)$ to the origin.

4 Design of control law

In this section, the design procedure of the proposed steering control law is described. The authors first describe a conventional method and its problem in Sect. 4.1. This is designed by considering a cascade system composed of kinematics Eq. 3, dynamics Eq. 4, and sometimes a rudder manipulation system Eq. 10. Next, in Sect. 4.2, the authors propose the expression of state variables with tanh function and auxiliary variables to guarantee the satisfaction of input constraints. Moreover, based on this expression, an unconstrained strict-feedback system [30] is derived. Then, in Sect. 4.3, the control input for $\psi^d(t)$ satisfying Eqs. 15 and 16 is constructed based on the backstepping method [30, 31], and the exponential stability is proven in Sect. 4.4.

It should be noted that, in the proposed method, it is assumed that the tracking of $\psi^d(t)$ is possible with mild rudder manipulation. This point is detailed in Sect. 6.

In the following, (t), which indicates the dependence of variables on time, is omitted to simplify the description.

4.1 Conventional method

Without input constraints Eqs. 8 and 9, it is known that a steering control that achieves the control objective, i.e., exponentially stabilizes the tracking error at the origin, can be designed by applying the backstepping method to cascade systems, for instance, kinematics Eq. 3 and dynamics Eq. 4. This method is described below. The time derivative of e_ψ is calculated with Eq. 3 as:

$$\dot{e}_\psi = r - \dot{\psi}^d. \tag{18}$$

Here an error variable $e_r := r - \{-c_1 e_\psi - (-\dot{\psi}^d)\}$ is defined with $c_1 > 0$. With e_r, Eq. 18 is written as:

$$\dot{e}_\psi = -c_1 e_\psi + e_r. \tag{19}$$

The time derivative of e_r is calculated as:

$$\dot{e}_r = f(r) + b\delta + c_1(r - \dot{\psi}^{\mathrm{d}}) - \ddot{\psi}^{\mathrm{d}}. \tag{20}$$

The control law:

$$\delta = \alpha_\delta(\psi, r, \psi^{\mathrm{d}}, \dot{\psi}^{\mathrm{d}}, \ddot{\psi}^{\mathrm{d}}) \tag{21}$$

is designed as:

$$\begin{aligned}&\alpha_\delta(\psi, r, \psi^{\mathrm{d}}, \dot{\psi}^{\mathrm{d}}, \ddot{\psi}^{\mathrm{d}})\\ &\quad := \frac{1}{b}\left[-c_2 e_r - e_\psi - \left\{f(r) + c_1(r - \ddot{\psi}^{\mathrm{d}}) - \ddot{\psi}^{\mathrm{d}}\right\}\right]\end{aligned} \tag{22}$$

with $c_2 > 0$. Then, Eq. 20 becomes:

$$\dot{e}_r = -c_2 e_r - e_\psi. \tag{23}$$

Now, an error variable:

$$e := (e_\psi \;\; e_r)^\top \in \mathbb{R}^2 \tag{24}$$

is defined. In addition, a function $V_e : \mathbb{R}^2 \to \mathbb{R}$ is defined as:

$$V_e := \frac{1}{2} e^\top e > 0, \quad \forall e \neq 0. \tag{25}$$

With Eqs. 19 and 23, the system for e is derived as:

$$\dot{e} = -C_e e + S_e e, \tag{26}$$

where

$$C_e := \mathrm{diag}(c_1, c_2), \tag{27}$$

$$S_e := \begin{pmatrix} 0 & 1 \\ -1 & 0 \end{pmatrix}. \tag{28}$$

With Eq. 26, the time derivative of V_e is calculated as:

$$\begin{aligned}\dot{V}_e &= e^\top \dot{e}\\ &= e^\top(-C_e e + S_e e)\\ &= -e^\top C_e e < 0 \quad \forall e \neq 0.\end{aligned} \tag{29}$$

Now it is shown that V_e is a global Lyapunov function [35] on $\mathbb{R}^2$. That is, if no constraints are imposed on the input, this method can make e globally exponentially stable at the origin. Thus, the goal of the control design has been achieved.

However, the steering control α_δ may not achieve the control objective if it is implemented in the system with constraints Eqs. 8 and 9. α_δ may output the command that does not satisfy the Eqs. 8 and 9. In many cases, for a given command from α_δ, δ and $\dot{\delta}$ are determined based on:

$$\delta = \mathrm{sat}(\alpha_\delta(\cdot), M), \tag{30}$$

$$\dot{\delta} = \mathrm{sat}(\dot{\alpha}_\delta(\cdot), R). \tag{31}$$

In the case saturation occurs in these processes, the desired performance may not be achieved as indicated in [8, 9].

4.2 Auxiliary system for input constraints

To deal with Eq. 8, tanh function and an auxiliary variable are introduced, as some existing method [14, 25, 28, 29], and an auxiliary system is derived. The rudder angle is expressed as:

$$\delta = M \tanh(k_\delta \widetilde{\delta}), \tag{32}$$

with $k_\delta > 0$ and an auxiliary variable $\widetilde{\delta} \in \mathbb{R}$. The time derivative of Eq. 32 is calculated, using the fundamental feature of tanh function, as:

$$\begin{aligned}\dot{\delta} &= M(1 - \tanh^2(k_\delta \widetilde{\delta}))k_\delta \dot{\widetilde{\delta}}\\ &= k_\delta M\left\{1 - \left(\frac{\delta}{M}\right)^2\right\}\dot{\widetilde{\delta}}\\ &= k_\delta \frac{M^2 - \delta^2}{M}\dot{\widetilde{\delta}}.\end{aligned} \tag{33}$$

Defining a function $g_\delta : \mathbb{R} \to \mathbb{R}$ as:

$$g_\delta(\delta) := k_\delta \frac{M^2 - \delta^2}{M}, \tag{34}$$

Eq. 33 becomes:

$$\dot{\delta} = g_\delta(\delta)\dot{\widetilde{\delta}}. \tag{35}$$

Here, new auxiliary state variable $\xi := \dot{\widetilde{\delta}}$ is introduced. In the following, it is assumed that the value $M^2 - \delta^2 > 0$ is enough large, that is the value of $g_\delta(\delta)$ is enough larger than zero. This assumption is for the avoidance of the numerical overflow in the controlled system, which is detailed in Sect. 6.

With Eq. 35, the constraint on rudder manipulation speed Eq. 9 is converted as:

$$\begin{aligned}&k_\delta \frac{M^2 - \delta^2}{M}|\xi| \le R \quad \forall t\\ \Leftrightarrow \quad &|\xi| \le \frac{MR}{k_\delta(M^2 - \delta^2)} \quad \forall t.\end{aligned} \tag{36}$$

To guarantee the satisfaction of the constraint on ξ Eq. 36, tanh function and an auxiliary variable are again introduced. ξ is expressed as:

$$\xi = \frac{MR}{k_\delta(M^2 - \delta^2)} \tanh(k_\xi \widetilde{\xi}), \tag{37}$$

with $k_\xi > 0$ and an auxiliary variable $\widetilde{\xi} \in \mathbb{R}$. Using Eqs. 33 and 37, the time derivative of Eq. 37 is calculated as:

$$\begin{aligned}
\dot{\xi} &= \frac{\mathrm{d}}{\mathrm{d}\delta}\left\{\frac{MR}{k_\delta(M^2-\delta^2)}\right\}\cdot\dot{\delta}\cdot\tanh(k_\xi\widetilde{\xi}) \\
&\quad + \frac{MR}{k_\delta(M^2-\delta^2)}\cdot\frac{\mathrm{d}}{\mathrm{d}t}\left\{\tanh(k_\xi\widetilde{\xi})\right\} \\
&= \frac{2MR\delta}{k_\delta(M^2-\delta^2)^2}\cdot k_\delta\frac{M^2-\delta^2}{M}\xi\cdot\frac{k_\delta(M^2-\delta^2)}{MR}\xi \\
&\quad + \frac{MR}{k_\delta(M^2-\delta^2)}\cdot\{1-\tanh^2(k_\xi\widetilde{\xi})\}k_\xi\dot{\widetilde{\xi}} \\
&= \frac{2k_\delta\delta\xi^2}{M} \\
&\quad + \frac{MR}{k_\delta(M^2-\delta^2)}\left[1-\left\{\frac{k_\delta(M^2-\delta^2)}{MR}\xi\right\}^2\right]k_\xi\dot{\widetilde{\xi}} \\
&= \frac{2k_\delta\delta\xi^2}{M} + \frac{MR}{k_\delta(M^2-\delta^2)} \\
&\quad \times\left\{\frac{k_\delta(M^2-\delta^2)}{MR}\right\}^2\left[\left\{\frac{MR}{k_\delta(M^2-\delta^2)}\right\}^2-\xi^2\right]k_\xi\dot{\widetilde{\xi}} \\
&= \frac{2k_\delta\delta\xi^2}{M} \\
&\quad + \frac{k_\delta k_\xi(M^2-\delta^2)}{MR}\left[\left\{\frac{MR}{k_\delta(M^2-\delta^2)}\right\}^2-\xi^2\right]\dot{\widetilde{\xi}} \\
&= f_\xi(\delta,\xi) + g_\xi(\delta,\xi)\dot{\widetilde{\xi}},
\end{aligned} \tag{38}$$

where

$$\begin{cases}
f_\xi(\delta,\xi) := \dfrac{2k_\delta\delta\xi^2}{M} \\
g_\xi(\delta,\xi) := \dfrac{k_\delta k_\xi(M^2-\delta^2)}{MR}\left[\left\{\dfrac{MR}{k_\delta(M^2-\delta^2)}\right\}^2-\xi^2\right].
\end{cases} \tag{39}$$

Here, new auxiliary variable $\eta := \dot{\widetilde{\xi}}$ is introduced as the input. In the following, it is assumed that the value $[MR/\{k_\delta(M^2-\delta^2)\}]^2 - \xi^2$ is enough large, that is, the value of $g_\xi(\delta,\xi)$ is enough larger than zero. This assumption is also for the avoidance of the numerical overflow in the controlled system, which is detailed in Sect. 6.

Now, the whole system with the states ψ, r, δ, ξ and the input η is described as a cascade system:

$$\begin{cases}
\dot{\psi} = r \\
\dot{r} = f(r) + b\delta \\
\dot{\delta} = g_\delta(\delta)\xi \\
\dot{\xi} = f_\xi(\delta,\xi) + g_\xi(\delta,\xi)\eta.
\end{cases} \tag{40}$$

It should be noted that:

$$\begin{cases}
g_\delta(\delta) \neq 0 \\
g_\xi(\delta,\xi) \neq 0
\end{cases} \quad \forall t. \tag{41}$$

This is because we have

$$|\delta| < M \quad \forall t, \tag{42}$$

$$|\dot{\delta}| < R \quad \forall t, \tag{43}$$

due to Eqs. 32 and 37, respectively. This means that the satisfaction of constraints Eqs. 8 and 9 is guaranteed in Eq. 40. In addition, Eq. 40 has the strict-feedback form [30], where all the state equations have the input-affine form and are described by state variables that appear above and input. Here, the problem defined in Sect. 3 is transformed into the tracking problem for Eq. 40 without any constraints on input η.

4.3 Design of control input

In this section, the design of the proposed control input $\eta = \alpha_\eta(\cdot)$ is described. Due to the feature of the introduced cascade system Eq. 40, α_η can be designed using the backstepping method [30, 31]. In the following, the arguments of functions: r, δ, and ξ are omitted to simplify the description.

The following error variables are defined.

$$\begin{cases}
z_1 := e_\psi & \text{(44a)} \\
z_2 := r - \alpha_1 & \text{(44b)} \\
z_3 := b\delta - \alpha_2 & \text{(44c)} \\
z_4 := bg_\delta\xi - \alpha_3 & \text{(44d)}
\end{cases}$$

In Eq. 44, signals α_1, α_2, and α_3 are interpreted as the target signals for r, $b\delta$, and $bg_\delta\xi$, respectively. The proposed control input α_η and these target signals are designed step by step in the following.

Step 1

The time derivative of Eq. 44a yields

$$\dot{z}_1 = r - \dot{\psi}^{\mathrm{d}}. \tag{45}$$

A candidate Lyapunov function

$$V_1 := \frac{1}{2} z_1^2 \tag{46}$$

is considered for the control design for z_1. Using, Eq. 45, the time derivative of V_1 is calculated as

$$\dot{V}_1 = z_1(r - \dot{\psi}^{\mathrm{d}}). \tag{47}$$

With Eq. 47, an ideal value of r is designed as

$$r = -c_1 z_1 - (-\dot{\psi}^{\mathrm{d}}) \tag{48}$$

with a design parameter $c_1 > 0$. This is motivated by the fact that, if Eq. 48 stands, the time derivative of V_1 becomes

$$\dot{V}_1 = -c_1 z_1^2, \tag{49}$$

which means the error variable z_1 is stabilized. Thus, the target signal for r is designed as

$$\alpha_1 = -c_1 z_1 - (-\dot{\psi}^{\mathrm{d}}). \tag{50}$$

Since the state r cannot be determined arbitrarily, Eq. 48 is achieved indirectly. By using the second error variable z_2 to express r, Eqs. 45 and 47 become

$$\dot{z}_1 = -c_1 z_1 + z_2 \tag{51}$$

and

$$\dot{V}_1 = -c_1 z_1^2 + z_1 z_2, \tag{52}$$

respectively. For the establishment of Eq. 48, in other words, for the regulation of the error variable z_2, the second target signal α_2 is designed in the next step.

Step 2

The time derivative of Eq. 44b yields

$$\dot{z}_2 = c_1(r - \dot{\psi}^{\mathrm{d}}) + f + b\delta - \ddot{\psi}^{\mathrm{d}}. \tag{53}$$

A candidate Lyapunov function

$$V_2 := V_1 + \frac{1}{2} z_2^2 \tag{54}$$

is considered for the control design for z_2. Using, Eq. 53, the time derivative of V_2 is calculated as

$$\dot{V}_2 = -c_1 z_1^2 + z_1 z_2 + z_2\{c_1(r - \dot{\psi}^{\mathrm{d}}) + f + b\delta - \ddot{\psi}^{\mathrm{d}}\}. \tag{55}$$

With Eq. 55, an ideal value of $b\delta$ is designed as

$$b\delta = -c_2 z_2 - z_1 - \{c_1(r - \dot{\psi}^{\mathrm{d}}) + f - \ddot{\psi}^{\mathrm{d}}\} \tag{56}$$

with a design parameter $c_2 > 0$. This is motivated by the fact that, if Eq. 56 stands, the time derivative of V_2 becomes

$$\dot{V}_1 = -c_1 z_1^2 - -c_2 z_2^2, \tag{57}$$

which means the error variables z_1 and z_2 are stabilized. Thus, the target signal for $b\delta$ is designed as

$$\alpha_2 = -c_2 z_2 - z_1 - \{c_1(r - \dot{\psi}^{\mathrm{d}}) + f - \ddot{\psi}^{\mathrm{d}}\}. \tag{58}$$

Since the state δ cannot be determined arbitrarily in the state equation Eq. 40, Eq. 56 is achieved indirectly. By using the third error variable z_3 to express $b\delta$, Eqs. 53 and 55 become

$$\dot{z}_2 = -c_2 z_2 - z_1 + z_3 \tag{59}$$

and

$$\dot{V}_2 = -c_1 z_1^2 - c_2 z_2^2 + z_2 z_3, \tag{60}$$

respectively. For the establishment of Eq. 56, in other words, for the regulation of the error variable z_3, the second target signal α_3 is designed in the next step.

Step 3

The time derivative of Eq. 44c yields

$$\begin{aligned}\dot{z}_3 = {} & (c_1 c_2 + 1)(r - \dot{\psi}^{\mathrm{d}}) + (c_1 + c_2)\left(f + b\delta - \ddot{\psi}^{\mathrm{d}}\right) \\ & + \frac{\mathrm{d}f}{\mathrm{d}r}(f + b\delta) + b g_\delta \xi - \dddot{\psi}^{\mathrm{d}}.\end{aligned} \tag{61}$$

A candidate Lyapunov function

$$V_3 := V_2 + \frac{1}{2} z_3^2 \tag{62}$$

is considered for the control design for z_3. Using, Eq. 61, the time derivative of V_3 is calculated as

$$\begin{aligned}\dot{V}_3 = {} & -c_1 z_1^2 - c_2 z_2^2 + z_2 z_3 \\ & + z_3\Big\{(c_1 c_2 + 1)\left(r - \dot{\psi}^{\mathrm{d}}\right) \\ & \quad + (c_1 + c_2)\left(f + b\delta - \ddot{\psi}^{\mathrm{d}}\right) \\ & \quad + \frac{\mathrm{d}f}{\mathrm{d}r}(f + b\delta) + b g_\delta \xi - \dddot{\psi}^{\mathrm{d}}\Big\}.\end{aligned} \tag{63}$$

With Eq. 63, an ideal value of $b g_\delta \xi$ is designed as

$$
\begin{aligned}
bg_\delta\xi =& -c_3z_3 - z_2 \\
&- \Big\{(c_1c_2+1)(r-\dot{\psi}^{\mathrm{d}}) \\
&\quad + (c_1+c_2)\big(f+b\delta-\ddot{\psi}^{\mathrm{d}}\big) \\
&\quad + \frac{\mathrm{d}f}{\mathrm{d}r}(f+b\delta) + bg_\delta\xi - \dddot{\psi}^{\mathrm{d}}\Big\}
\end{aligned} \tag{64}
$$

with a design parameter $c_3 > 0$. This is motivated by the fact that, if Eq. 64 stands, the time derivative of V_3 becomes

$$
\dot{V}_3 = -c_1z_1^2 - c_2z_2^2 - c_3z_3^2, \tag{65}
$$

which means the error variables z_1, z_2, and z_3 are stabilized. Thus, the target signal for $bg_\delta\xi$ is designed as

$$
\begin{aligned}
\alpha_3 =& -c_3z_3 - z_2 \\
&- \Big\{(c_1c_2+1)(r-\dot{\psi}^{\mathrm{d}}) \\
&\quad + (c_1+c_2)\big(f+b\delta-\ddot{\psi}^{\mathrm{d}}\big) \\
&\quad + \frac{\mathrm{d}f}{\mathrm{d}r}(f+b\delta) + bg_\delta\xi - \dddot{\psi}^{\mathrm{d}}\Big\}.
\end{aligned} \tag{66}
$$

Since the states δ and ξ cannot be determined arbitrarily in the state equation Eq. 40, Eq. 64 is achieved indirectly. By using the fourth error variable z_4 to express $bg_\delta\xi$, Eqs. 61 and 63 become

$$
\dot{z}_3 = -c_3z_3 - z_2 + z_4 \tag{67}
$$

and

$$
\dot{V}_3 = -c_1z_1^2 - c_2z_2^2 - c_3z_3^2 + z_3z_4, \tag{68}
$$

respectively. For the establishment of Eq. 64, in other words, for the regulation of the error variable z_4, the control input α_η is designed in the next step.

Step 4

The time derivative of Eq. 44d yields

$$
\begin{aligned}
\dot{z}_4 =& (c_1+c_3+c_1c_2c_3)(r-\dot{\psi}^{\mathrm{d}}) \\
&+ (c_1c_2+c_2c_3+c_3c_1+2)(f+b\delta-\ddot{\psi}^{\mathrm{d}}) \\
&+ (c_1+c_2+c_3)\Big\{\frac{\mathrm{d}f}{\mathrm{d}r}(f+b\delta) + bg_\delta\xi - \dddot{\psi}^{\mathrm{d}}\Big\} \\
&+ \frac{\mathrm{d}^2f}{\mathrm{d}r^2}(f+b\delta)^2 + \frac{\mathrm{d}f}{\mathrm{d}r}\Big\{\frac{\mathrm{d}f}{\mathrm{d}r}(f+b\delta) + bg_\delta\xi\Big\} \\
&+ b\Big\{\frac{\mathrm{d}g_\delta}{\mathrm{d}\delta}g_\delta\xi^2 + g_\delta(f_\xi + g_\xi\eta)\Big\} - \dddot{\psi}^{\mathrm{d}}.
\end{aligned} \tag{69}
$$

Following a similar procedure as Steps 1, 2, and 3, the control input is designed as

$$
\begin{aligned}
\alpha_\eta =& \frac{1}{bg_\delta g_\xi}\Bigg(- c_4z_4 - z_3 \\
&- \Big[(c_1+c_3+c_1c_2c_3)(r-\dot{\psi}^{\mathrm{d}}) \\
&\quad + (c_1c_2+c_2c_3+c_3c_1+2)(f+b\delta-\ddot{\psi}^{\mathrm{d}}) \\
&\quad + (c_1+c_2+c_3)\Big\{\frac{\mathrm{d}f}{\mathrm{d}r}(f+b\delta) + bg_\delta\xi - \dddot{\psi}^{\mathrm{d}}\Big\} \\
&\quad + \frac{\mathrm{d}^2f}{\mathrm{d}r^2}(f+b\delta)^2 + \frac{\mathrm{d}f}{\mathrm{d}r}\Big\{\frac{\mathrm{d}f}{\mathrm{d}r}(f+b\delta) + bg_\delta\xi\Big\} \\
&\quad + b\Big\{\frac{\mathrm{d}g_\delta}{\mathrm{d}\delta}g_\delta\xi^2 + g_\delta f_\xi\Big\} - \dddot{\psi}^{\mathrm{d}}\Big]\Bigg) \\
=& \frac{1}{bg_\delta g_\xi}\Bigg(\\
&- (c_1c_2 + c_3c_4 + c_4c_1 \\
&\qquad + c_1c_2c_3c_4 + 1)(\psi - \psi^{\mathrm{d}}) \\
&- (2c_1 + c_2 + c_3 + 2c_4 + c_1c_2c_3 \\
&\qquad + c_4c_1c_2 + c_3c_4c_1 + c_2c_3c_4)(r - \dot{\psi}^{\mathrm{d}}) \\
&- (c_1c_2 + c_1c_3 + c_1c_4 \\
&\qquad + c_2c_3 + c_2c_4 + c_3c_4 + 3)(f + b\delta - \ddot{\psi}^{\mathrm{d}}) \\
&- (c_1 + c_2 + c_3 + c_4) \\
&\quad \times \Big\{\frac{\mathrm{d}f}{\mathrm{d}r}(f+b\delta) + bg_\delta\xi - \dddot{\psi}^{\mathrm{d}}\Big\} \\
&- \Big[\frac{\mathrm{d}^2f}{\mathrm{d}r^2}(f+b\delta)^2 + \frac{\mathrm{d}f}{\mathrm{d}r}\Big\{\frac{\mathrm{d}f}{\mathrm{d}r}(f+b\delta) + bg_\delta\xi\Big\} \\
&\quad + b\Big\{\frac{\mathrm{d}g_\delta}{\mathrm{d}\delta}g_\delta\xi^2 + g_\delta f_\xi\Big\} - \dddot{\psi}^{\mathrm{d}}\Big]\Bigg),
\end{aligned} \tag{70}
$$

with a design parameter $c_4 > 0$. By substituting Eq. 70, Eq. 69 becomes

$$
\dot{z}_4 = -c_4z_4 - z_3. \tag{71}
$$

4.4 Exponential stability

In this section, the exponential stability of the tracking error at the origin ($e_\psi = 0$) is presented for the feasible target signal.

The error variable $z := (z_1\ z_2\ z_3\ z_4)^\top$ and a candidate Lyapunov function:

$$
V(z) := \frac{1}{2}z^\top z > 0 \quad \forall z \neq 0 \tag{72}
$$

Fig. 4 Photograph of the subject ship

are defined. With Eqs. 51, 59, 67 and 71, the system of z is described as:

$$\dot{z} = -Cz + Sz, \tag{73}$$

where

$$C := \mathrm{diag}(c_1, c_2, c_3, c_4), \tag{74}$$

$$S := \begin{pmatrix} 0 & 1 & 0 & 0 \\ -1 & 0 & 1 & 0 \\ 0 & -1 & 0 & 1 \\ 0 & 0 & -1 & 0 \end{pmatrix}. \tag{75}$$

Therefore the time derivative of V is:

$$\begin{aligned} \dot{V} &= z^{\mathrm{T}}\dot{z} \\ &= z^{\mathrm{T}}(-Cz + Sz) \\ &= -z^{\mathrm{T}}Cz < 0 \quad \forall z \neq 0. \end{aligned} \tag{76}$$

Thus, it is proven that, if Eqs. 15 and 16 are satisfied, then z is locally uniformly exponentially stable at the origin.

5 Numerical experiments

The proposed method was verified in the numerical experiments of the target heading angle tracking control. In this study, experiments in a real environment using the subject ship were not implemented because the proposed control law is sufficiently verified by numerical experiments. The proposed control law guarantees control performance with respect to the target system, including a response model expressed in cubic form. To illustrate or verify this, simulations of the maneuvering motion subject to the target system are sufficient.

5.1 Setting

The subject ship was a model ship of *M.V. ESSO OSAKA* (Fig. 4). A nonlinear maneuvering model Eq. 6 was adopted in the numerical experiments. The parameters of the maneuvering model Eq. 6, the limits on the constraints Eqs. 8 and 9 are summarized in Tables 1 and 2, respectively. The parameters in Table 1 are determined by the system identification method using time series data of the free-running tests of the subject ship. The limits on the constraints; M and R were determined based on the mechanical constraints of the subject ship. The design parameters in the derived cascade system Eq. 40 and in the controller α_η are chosen as $k_\delta = k_\xi = 1$ and $c_1 = c_2 = c_3 = c_4 = 1$. The time series were calculated by the Euler method for Case1 and by the Euler–Maruyama method for Case2. In all numerical simulations, the time width $\Delta t = 0.01$ s was set. Initial states were set as $\psi(0) = r(0) = \delta(0) = \xi(0) = 0$ in Case1 and 2.

The proposed steering control law was applied for these two cases.

5.1.1 Case1: heading tracking

In Case1, the proposed steering control law was applied for heading tracking control. The proposed control law is designed for the tracking control with input magnitude and rate which freely behave within the constraints. However, with the current techniques of the authors, the computational problem with numerical saturation in the proposed method, which is detailed in Sect. 6, cannot be solved. Therefore, in this case, the following smooth function was adopted as the target signal.

$$\psi^{\mathrm{d}}(t) = \frac{1}{2}\Psi^{\mathrm{d}}\left(1 + \tanh\frac{t - t_{\tanh}}{d_{\tanh}}\right), \tag{77}$$

where $t_{\tanh} = 5 + 0.3\Psi^{\mathrm{d}}$, $d_{\tanh} = 2.5 + 0.15\Psi^{\mathrm{d}}$, and Ψ^{d} is the value of $\psi^{\mathrm{d}}(t)$ at $t \to \infty$. Five scenarios with $\Psi^{\mathrm{d}} = 10, 20, 30, 40, 50$ were simulated.

Table 2 Threshold values of constraints (Eqs. 8 and 9) considered in the numerical simulation

Item	M [deg]	R [deg/s]
Value	35	20

Table 1 Parameters of maneuvering model used in the numerical simulation

Item	K	T	n_0	n_1	n_2	n_3
Value	0.21	8.8	0	0.41	0	0.23

5.1.2 Case2: course keeping under disturbance

In Case2, the proposed steering control law was applied for course keeping control under stochastic disturbance to check the robustness of the proposed method. The reference signal was set as $\psi^{\mathrm{d}}(t) = 0$. In Case2, the following system having the form of stochastic differential equation (SDE) was considered:

$$\mathrm{d}r(t) = \big(f(r(t)) + b\delta(t)\big)\mathrm{d}t + \sigma \mathrm{d}W(t), \tag{78}$$

where the Weiner process was introduced as additive noise to the model Eq. 4 with $\sigma > 0$. Therefore, the inclusion of Wong–Zakai correction term is not necessary. This noise can be considered as a modeling error, external disturbance such as wind, or observation noise. In this study, we set $\sigma = bM = 0.835$, which is equivalent to the maximum influence of rudder force on the $\dot{r}$. Equation 78 was numerically solved by the Euler–Maruyama method:

$$\begin{aligned} r(t + \Delta t) = r(t) + \big(f(r) + b\delta(t)\big)\Delta t \\ + \sigma(W(t + \Delta t) - W(t)), \end{aligned} \tag{79}$$

where $(W(t + \Delta t) - W(t))$ follows the normal distribution:

$$\mathcal{N}(0, \Delta t) = \sqrt{\Delta t}\mathcal{N}(0, 1). \tag{80}$$

5.2 Result

5.2.1 Case1: Heading tracking

The time series simulated in Case1 is shown in Fig. 5. In Case1, the proposed steering control law was applied for heading tracking control where the target signal is formulated as Eq. 77. From Fig. 5, it is confirmed that, for every case of heading change angle Ψ^{d}, both signals of δ and $\hat{\delta}$ did not break the constraints Eqs. 8 and 9, and the heading angle ψ successfully tracked the target signal ψ^{d}. This result verifies the performance of the proposed steering control law for a mild target signal.

5.2.2 Case2: Course keeping under disturbance

The time series simulated in Case2 is shown in Fig. 6.

In Case2, the proposed steering control law was applied for course keeping control under stochastic disturbance. Stochastic noise can be observed in the time series of r. Even with this stochastic noise, the course deviation was successfully controlled with the proposed method within the input magnitude and rate constraints. This result shows the robustness of the proposed method to stochastic noise to some extent.

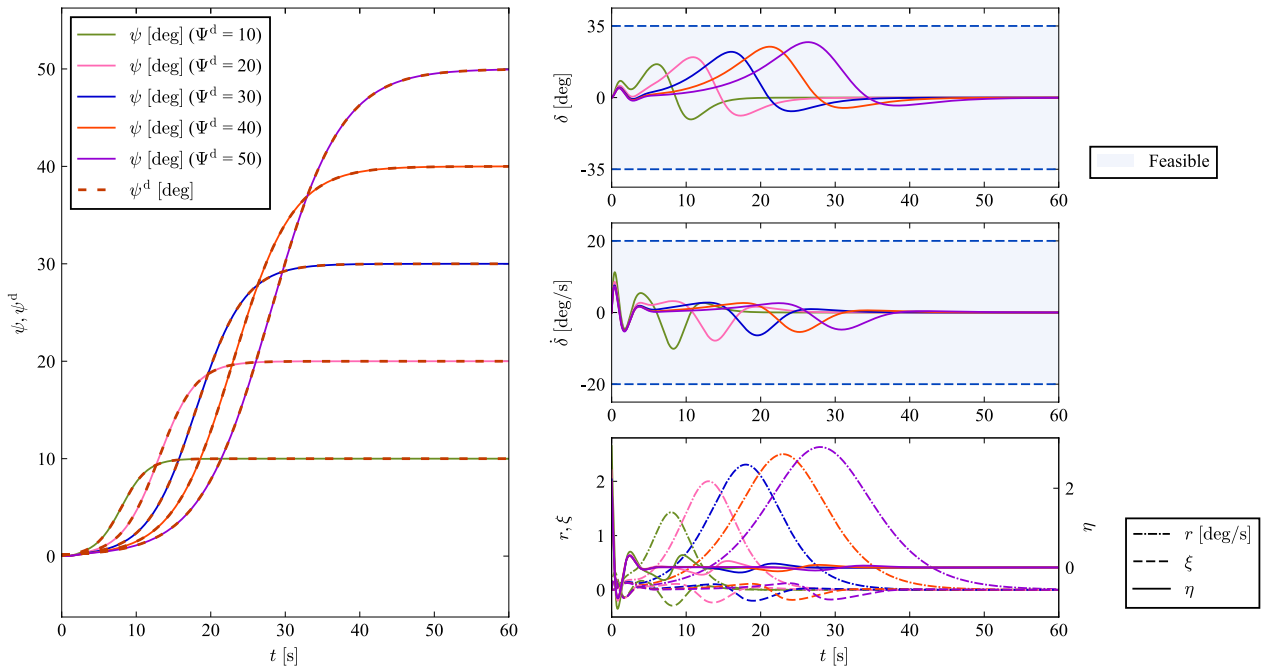

Fig. 5 Case1. The proposed control law was applied for heading tracking control. The target signal $\psi^{\mathrm{d}}(t)$ was Eq. 77

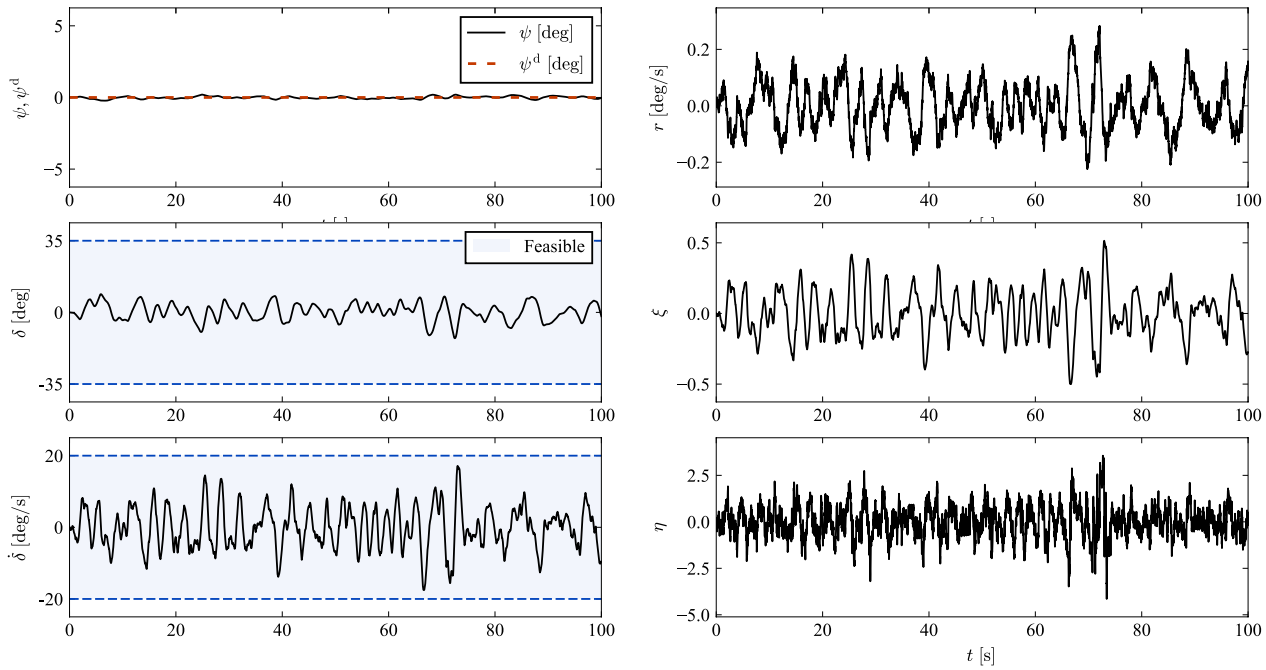

Fig. 6 Case2. The proposed control law was implemented in the course keeping control with external disturbance

6 Discussion and limitation

The approximation of the response of maneuvering motion by the function of Eq. 6 has achieved a certain degree of reliability [33]. The proposed control law is novel in that, based on this model, it makes the error system exponentially stable while guaranteeing the satisfaction of the constraints of rudder angle and steering speed. The proposed control law does not guarantee a certain control performance in a real environment where wind, waves, and currents affect the ship's motion. However, it is expected that following future research will allow the proposed control law to be developed in terms of adaptability and robustness. The outcome of these future studies will provide a guarantee for control performance in real environments based on control theory and high control performance in experiments in real environments using real- or model-scaled ships.

The proposed steering control law can achieve heading tracking with exponential convergence of tracking error under the constraints of rudder angle and steering speed, as shown in Sect. 4.4. Theoretically, the proposed method enables the tracking control that makes full use of almost all feasible magnitude and rate of rudder manipulation. In addition, due to the formulation Eqs. 32 and 37, the auxiliary system introduced by the authors has a mechanism to avoid saturation of input magnitude and rate, and δ and $\dot{\delta}$ never reach the thresholds of constraints.

However, the proposed method has drawbacks in terms of numerical implementation. The cascade system Eq. 40 and the controller α_η are valid as long as the states δ and $\dot{\delta}$ are not too close to the thresholds of the constraints Eqs. 8 and 9. However, the authors found that in the case these states get too close to the thresholds, effective solutions are unavailable. This is because the proposed control method does not ensure the boundedness of all signals in the closed loop. For example, in the third equation of Eq. 40, as ξ that makes $|\delta|$ approaches M continues to be input, the value of $g_\delta(\delta)$ approaches zero. This leads to the divergence of the right hand side of Eq. 40 and the output of the controller Eq. 70. As a result, due to numerical overflow, a time series cannot be obtained unless the time width is infinitely small. Such control would be performed in the case a large rudder angle or/and rapid manipulation of the rudder is required, such as a large angle change of heading. This problem can be avoided to some extent by tuning design parameters c_i $(i = 1, 2, 3, 4)$. At the present stage, it is better to shape a smooth reference signal for course change control, as exemplified in Case1 (Fig. 5). Future work includes improving the design of control law and numerical processing to obtain a steering control law that overcomes this limitation.

7 Conclusion

A ship steering control law for a nonlinear system with constraints of both input magnitude and rate is proposed. The satisfaction of all input constraints is guaranteed by introducing a bounded smooth tanh function and auxiliary variables. Furthermore, using the feature of the derivative of tanh function, the time derivatives of the newly formulated state variables are calculated without auxiliary variables, and a strict-feedback system without any input constraints is derived. The control input is designed based on the backstepping method, and the local exponential stability of the tracking error is proven. In the numerical experiments, it is shown that the proposed control law successfully avoids saturation of input magnitude and rate and achieves the tracking of the target heading angle. The unboundedness of the auxiliary systems and the constructed control law limit the proposed method, and these problems will be treated in future studies.

Acknowledgements This study was supported by a Grant-in-Aid for Scientific Research from the Japan Society for Promotion of Science (JSPS KAKENHI Grant #22H01701). The study also received assistance from the Fundamental Research Developing Association for Shipbuilding and Offshore (REDAS) in Japan (REDAS23-5(18A)). Finally, the authors would like to thank Prof. Naoya Umeda, Asst. Prof. Masahiro Sakai, Osaka University, and Prof. Hiroyuki Kajirawa, Kyushu University, for technical discussion.

Funding Open Access funding provided by Osaka University.

Declarations

Conflict of interest The authors declare that they have no conflict of interest.

References

1. Tani H (1952) The course-keeping quality of a ship in steered conditions. J Zosen Kiokai 1952:25 **(in Japanese)**
2. van Amerongen J (1982) Adaptive steering of ships—a model-reference approach to improved manoeuvring and economical course keeping. Ph.D. thesis, Delft University of Technology
3. Minorsky N (1922) Directional stability of automatically steered bodies. J Am Soc Naval Eng 34(2):280
4. Schiff LI, Gimprich M (1949) Automatic steering of ships by proportional control. Trans Soc Nav Archit Mar Eng 57:94
5. Nomoto K, Taguchi K, Honda K, Hirano S (1957) On the steering qualities of ships. Int Shipbuild Prog 4(35):354
6. McGookin EW, Murray-Smith DJ, Li Y, Fossen TI (2000) Ship steering control system optimisation using genetic algorithms. Control Eng Pract 8(4):429
7. Du J, Guo C, Yu S, Zhao Y (2007) Adaptive autopilot design of time-varying uncertain ships with completely unknown control coefficient. IEEE J Ocean Eng 32(2):346
8. Doyle JC, Smith RS, Enns DF (1987) Control of plants with input saturation nonlinearities. In: 1987 American Control Conference
9. Yuan J, Chen YQ, Fei S (2018) Analysis of actuator rate limit effects on first-order plus time-delay systems under fractional-order proportional-integral control. IFAC-PapersOnLine 51(4):37
10. Duda H (1998) Flight control system design considering rate saturation. Aerosp Sci Technol 2(4):265
11. Kothare MV, Campo PJ, Morari M, Nett CN (1994) A unified framework for the study of anti-windup designs. Automatica 30(12):1869
12. Tarbouriech S, Turner M (2009) Anti-windup design: an overview of some recent advances and open problems. IET Control Theory Appl 3:1
13. Zhou J, Wen C (2006) Robust adaptive control of uncertain nonlinear systems in the presence of input saturation. IFAC Proc 39(1):149
14. Wen C, Zhou J, Liu Z, Su H (2011) Robust adaptive control of uncertain nonlinear systems in the presence of input saturation and external disturbance. IEEE Trans Autom Control 56(7):1672
15. Wang S, Gao Y, Liu J, Wu L (2018) Saturated sliding mode control with limited magnitude and rate. IET Control Theory Appl 12(8):1075
16. Sørensen MEN, Breivik M (2015) Comparing nonlinear adaptive motion controllers for marine surface vessels. IFAC-PapersOnLine 28:291
17. Breivik M, Strand JP, Fossen TI (2006) Guided dynamic positioning for fully actuated marine surface vessels. In: Proceedings of 7th IFAC Conference of Maneuvering Control, pp 1–6
18. Gaudio JE, Annaswamy AM, Bolender MA, Lavretsky E (2022) Adaptive flight control in the presence of limits on magnitude and rate. IEEE Access 10:65685
19. Sørensen MEN, Breivik M, Eriksen BOH (2017) A ship heading and speed control concept inherently satisfying actuator constraints. In: 1st Annual IEEE conference on control technology and applications, CCTA 2017 2017-Janua, p 323
20. Gou H, Guo X, Lou W, Ou J, Yuan J (2020) Path following control for underactuated airships with magnitude and rate saturation. Sensors (Switzerland) 20:1
21. Witkowska A, Tomera M, Śmierzchalski R (2007) A backstepping approach to ship course control. Int J Appl Math Comput Sci 17(1):73
22. Kahveci NE, Ioannou PA (2013) Adaptive steering control for uncertain ship dynamics and stability analysis. Automatica 49(3):685
23. Ejaz M, Chen M (2017) Sliding mode control design of a ship steering autopilot with input saturation. Int J Adv Robot Syst 14(3):1
24. Du J, Hu X, Sun Y (2017) Adaptive robust nonlinear control design for course tracking of ships subject to external disturbances and input saturation. IEEE Trans Syst Man Cybern Syst 50:193

25. Zhu L, Li T, Yu R, Wu Y, Ning J (2020) Observer-based adaptive fuzzy control for intelligent ship autopilot with input saturation. Int J Fuzzy Syst 22:1416
26. Fossen TI (2011) Handbook of marine craft hydrodynamics and motion control. Wiley, New York
27. Bemporad A (1998) Reference governor for constrained nonlinear systems. IEEE Trans Autom Control 43:415
28. Wang H, Chen B, Liu X, Liu K, Lin C (2013) Robust adaptive fuzzy tracking control for pure-feedback stochastic nonlinear systems with input constraints. IEEE Trans Cybern 43:2093
29. Zheng Z, Huang Y, Xie L, Zhu B (2018) Adaptive trajectory tracking control of a fully actuated surface vessel with asymmetrically constrained input and output. IEEE Trans Control Syst Technol 26:1851
30. Krstić M, Kanellakopoulos I, Kokotovic PV (1995) Nonlinear and adaptive control design. Wiley, New York
31. Fossen TI, Strand JP (1999) Tutorial on nonlinear backstepping: applications to ship control. https://doi.org/10.4173/mic.1999.2.3
32. Suyama R, Satoh S, Maki A (2023) Nonlinear autopilot in which constraints on magnitude and rate of steering are taken into account. In: The Japan Society of Naval Architects and Ocean Engineers 2023 Annual Spring Meeting, pp 11–20 (in Japanese)
33. Norrbin NH (1963) On the design and analysis of the zig-zag test on base of quasi-linear frequency response. In: Proceedings of the 10th International Towing Tank Conference, pp 355–374
34. Shouji K, Ohtsu K, Mizoguchi S (1992) An automatic berthing study by optimal control techniques. IFAC Proc Volumes 25(3):185
35. Khalil HK (1992) Nonlinear systems. Macmillan Publishing Company, New York